

# Development of high-speed quantum dots/graphene infrared detectors for uncooled infrared imaging

Judy Wu,<sup>1,2\*</sup> Maogang Gong,<sup>1,2</sup> Russell C. Schmitz,<sup>3</sup> Bo Liu<sup>2</sup>

<sup>1</sup>Zenoleap LLC, 2029 Becker Dr. Suite 100, Lawrence KS 66049

<sup>2</sup>Department of Physics and Astronomy, University of Kansas, Lawrence, KS 66045, USA

<sup>3</sup>U.S. Army DEVCOM C5ISR Center, Night Vision and Electronic Sensors Directorate, 10221 Burbeck Rd, Ft. Belvoir, 22060 VA, USA

## ABSTRACT

Colloidal semiconductor quantum dots/graphene van der Waals (vdW) heterojunctions take advantages of the enhanced light-matter interaction and spectral tunability of quantum dots (QDs) and superior charge mobility in graphene, providing a promising alternative for uncooled infrared photodetectors with a gain or external quantum efficiency up to  $10^{10}$ . In these QD/graphene vdW heterostructures, the QD/graphene interface plays a critical role in controlling the optoelectronic process including exciton dissociation, charge injection and transport. Specifically, charge traps at the vdW interface can increase the noise, reduce the responsivity and response speed. This paper highlight our recent progress in engineering the vdW heterojunction interface towards more efficient charge transfer for higher photoresponsivity,  $D^*$  and response speed. These results illustrate that the importance in vdW heterojunction interface engineering in QD/graphene photodetectors which may provide a promising pathway for low-cost, printable and flexible infrared detectors and imaging systems.

**Keywords:** Quantum dots, graphene, 2D atomic materials, van der Waals heterojunction, nanohybrids, infrared detectors

## 1. INTRODUCTION

Graphene regards a monolayer of carbon atoms arranged in a two-dimensional honeycomb lattice.<sup>1, 2</sup> Since its discovery in 2004, graphene has attracted a broad interest in both research and applications due to its superior physical properties including unique electronic structure, high charge carrier mobility, optical transparency, flexibility and chemical stability.<sup>3-9</sup> Specifically, graphene is a gapless, relativistic semiconductor or semimetal,<sup>10</sup> which implies that both electrons and holes can be described by a linear dispersion of  $E = \hbar v_F k$ , where the momentum-independent Fermi velocity  $v_F$  can be as high as 1/300 of the speed of light. This results in high carrier mobility ( $\mu$ ) that seems independent of temperature in a large range, independent of applied electric field, and is comparable for holes and electrons.<sup>4</sup> The intrinsic acoustic phonon limit of mobility is projected to be  $\sim 200,000 \text{ cm}^2/\text{V}\cdot\text{s}^{-1}$  at room temperature assuming a carrier density of  $(n) \sim 10^{12} \text{ cm}^{-2}$  at the charge neutrality or so-called Dirac point.<sup>4, 8</sup> Experimentally, high  $\mu$  up to  $\sim 15,000 \text{ cm}^2/\text{V}\cdot\text{s}^{-1}$  has been reported on graphene for both electrons and holes in the temperature range of 10-100 K, which could be further improved by eliminating extrinsic charge scattering mechanisms and defects in graphene. It should be pointed out that the carrier mobility in graphene is higher by many orders of magnitude than in metals and most semiconductors at room temperature. For example, crystalline Si has the electron and hole mobility of  $\sim 1400 \text{ cm}^2/\text{V}\cdot\text{s}^{-1}$  and  $450 \text{ cm}^2/\text{V}\cdot\text{s}^{-1}$ , respectively, at room temperature.

Graphene can be viewed as an atomically thin film available in large-area of centimeters in lateral dimension<sup>11</sup> and is compatible with conventional thin film-based microelectronics since the established microfabrication processes can be readily applied to make graphene circuits. This has motivated extensive exploration into graphene-based applications, such as optoelectronic nanohybrids photodetection, which consists of graphene and semiconductor nanostructures in heterostructures.<sup>12-14</sup> The nanostructures, such as quantum dots (QDs),<sup>13, 15-19</sup> nanotubes and nanowires (1D)<sup>20, 21</sup>, and nanosheets (2D) such as transition metal dichalcogenides (TMDCs)<sup>14, 22, 23</sup> serve as photosensitizers in the nanohybrids

photodetectors. The implementation of graphene of extraordinary charge carrier mobility in the nanohybrids makes a fundamental difference in the charge carrier transport in these nanohybrids photodetectors as compared to the counterparts based on the nanostructures only.

Colloidal QDs/graphene van der Waals (vdW) heterostructures have recently emerged as a promising scheme for photodetectors,<sup>13</sup> prompted by exciting progress made in colloidal QDs<sup>24</sup> and graphene.<sup>2-9</sup> As illustrated in **Figure 1**, the QD/graphene vdW heterostructure photodetectors differ from the graphene-only and QD-only counterparts. The graphene-only photodetector (**Figure 1a**) relies on light absorption and charge transport both by graphene. While graphene has a broad-band absorption from visible to mid-infrared,<sup>10, 25-27</sup> the limited absorption of 2.3% per graphene sheet would limit its responsivity to less than 20 mA/W under 100% external quantum efficiency (EQE).<sup>12</sup> In the QDs-only photodetectors, QDs are responsible for light absorption, while charge transport also occurs in the QD film (**Figure 1b**) which could be limited by the intra-QD low carrier mobility and the inter-QD junctions. The QDs-only photodetectors have been intensively studied, especially for infrared (IR) photodetection, in which the quantum confinement in QDs due to the suppressed phonon scattering<sup>28</sup> is expected to reduce dark current and hence improve the detector performance.<sup>29, 30</sup> This has been shown experimentally on colloidal HgTe QDs with surface passivation<sup>31-33</sup> and InSb-nanowires.<sup>34, 35</sup> However, the low carrier mobility, in the range of  $10^{-6}$  cm<sup>2</sup>V<sup>-1</sup>s<sup>-1</sup> (in as-made HgTe QDs) to  $10^{-4}$  cm<sup>2</sup>V<sup>-1</sup>s<sup>-1</sup> (with ligand exchange on HgTe QDs to passivate surface defects), remains to be addressed in order to achieve high figure-of-merit specific detectivity ( $D^*$ ) in QD-only photodetectors.<sup>33</sup> This issue can be addressed in QD/graphene vdW heterostructures photodetectors (**Figure 1c**) by enabling photocarrier transfer from QDs to graphene with a built-in electric field at the QD/graphene vdW interface. Charge transport in graphene between the electrodes takes advantages of the high mobility in graphene at room temperature. After the first report of PbS QD/graphene photodetectors by Konstantatos *et al* in 2012,<sup>13</sup> many QD/graphene vdW heterostructure photodetectors have been explored. In the QD/graphene vdW heterostructures, the QD photosensitizers absorb incident light, and the excitons generated in QDs could be dissociated by the built-in electric field at the QD/graphene interface, followed by charge transfer to graphene driven by the built-in field. The photoresponse is literally a photo-gating effect on graphene measured from the source and drain electrodes. High EQE or photoconductive gain up to  $10^{10}$ - $10^{12}$  can be achieved in QD/graphene vdW heterostructures photodetectors. The gain is defined as:  $\text{gain} = \tau_c / \tau_t$ <sup>13-15, 36-38</sup>, where  $\tau_c$  is the exciton life time in QDs and  $\tau_t$  is the carrier transit time defined as:  $\tau_t = L^2 / \mu V_{sd}$ . In a graphene channel of length  $L$  at a given source-drain bias voltage of  $V_{sd}$ ,  $\tau_t$  is inversely proportionate to the charge mobility  $\mu$  in graphene<sup>39</sup>. Thus the high EQE or gain in the QD/graphene vdW heterostructures photodetectors is a combination of the strong quantum confinement effects in QDs (high  $\tau_c$ ) and in graphene (low  $\tau_t$  due to high mobility  $\mu$ ),<sup>7, 8</sup> which has been demonstrated in various QD/graphene photodetectors.<sup>13, 14, 22, 23, 40-46</sup>

These advantages make QD/graphene nanohybrids highly promising for uncooled IR detectors that have been widely used in applications<sup>39, 47-50</sup> that require high detectivity, high speed, low-cost and scalability. For IR detection, colloidal QDs with a strong absorption in IR spectrum are typically adopted which include PbS, PbSe, HgTe, etc.<sup>51</sup> It should be pointed out that QDs have absorption spectra tunable by their size due to their bandgap dependence on QD size.<sup>52, 53</sup> Red shift in QDs, such as FeS<sub>2</sub>, has been observed via compositional tuning.<sup>18, 19</sup> However, the performance of the QD/graphene vdW heterostructures photodetectors depends sensitively on the QD surface states (defects, dangling bonds) and QD/graphene interface quality. This is not difficult to understand since both optical absorption, charge transfer from QDs to graphene and charge transport in graphene can be strongly affected by these surface and interface properties. For example, charge traps can form on the QD surface and QD/graphene interface, resulting in low photoresponse and response speed.<sup>54, 55</sup> For lower bandgap IR QDs, the effect of QD surface states can be more significant. Motivated by the need to optimize the QD surface and QD/graphene interface for both high photoresponse and fast photoresponse required for imaging systems, this paper reports a few schemes we have explored towards achieving a high-efficiency and high-speed charge transfer in QD/graphene vdW heterostructures photodetectors, especially in IR spectra. In the following, we will discuss our experimental results.

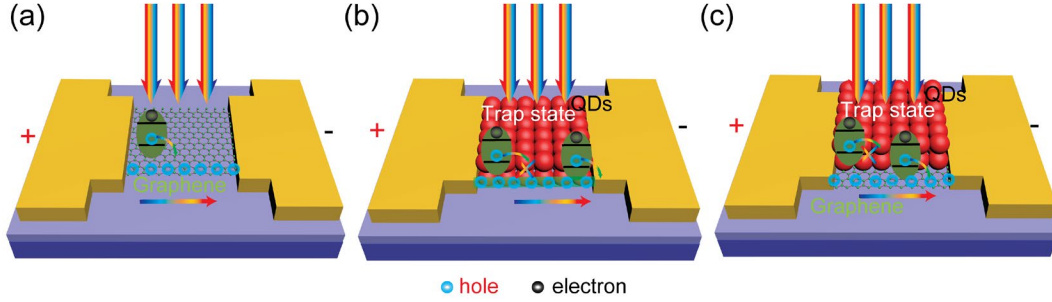


Figure 1. Schematic of (a) graphene-only (light absorption and charge transport in graphene channel), (b) QDs-only (light absorption and charge transport in QDs film channel) and (c) QD/graphene vdW heterostructures (light absorption by QDs, followed with charge transfer from QDs to graphene, and charge transport in graphene channel) photodetectors.

## 2. EXPERIMENTAL

Chemical vapor deposition (CVD) was used for synthesis of monolayer graphene in large area. It should be noted that the CVD graphene may be grown on commercial copper foils<sup>56, 57</sup> (to be resolved during transfer of graphene to other substrates)<sup>58</sup> and directly on SiO<sub>2</sub>/Si substrates (no graphene transfer is needed).<sup>59</sup> The advantage of the former is that graphene could be on a large variety of substrates, which is particularly important to those, such as polymers or plastics,<sup>60</sup> with a low thermal budgets incompatible to the CVD graphene growth temperatures typically exceeding 1000 °C. However, graphene transfer process is tedious and graphene could be contaminated by various chemical and solvent residues that can affect the QD/graphene interface through formation of charge scatters and charge traps. As we shall show later, such contaminations can degrade the performance of the QD/graphene vdW photodetectors by blocking the charge transfer (low responsivity and detectivity D\*) as well as forming charge traps that could slow down the photoresponse (asymmetric and large response times). Transfer-free, direct CVD growth of graphene can avoid the contamination of graphene. However, high quality CVD graphene has only been reported on a limited number of substrates that can sustain the CVD growth conditions for graphene, such as SiO<sub>2</sub>/Si, quartz and fused silica.

To make QD/graphene vdW heterostructure photodetectors, Au (40 nm)/Ti (10 nm) electrodes were fabricated either using e-beam evaporation or magnetron sputtering. Standard photolithography was employed to define the electrodes, followed with liftoff. Graphene channels were defined using the second photolithography, followed with reactive ion etch of graphene. The graphene channel dimension is 2-20  $\mu\text{m}$  (length) $\times$ 20  $\mu\text{m}$  (width).<sup>61</sup> For larger graphene channels of dimension > 100  $\mu\text{m}$ , shadow masks were used to define the electrodes and graphene channels.

Colloidal fabrication of QDs of various semiconductors have been intensively studied and the fabrication details can be found in our previous papers.<sup>15, 16, 45, 62</sup> Inks containing the fabricated colloidal QDs were prepared for inkjet printing of the QDs to graphene channels.<sup>63, 64</sup> It should be realized that QDs have a large surface to volume ratio because of their small dimensions on the order of few to few tens of nm. The large surface area on lowband gap semiconductor QDs implies surface defects that may cause degradation in ambient and poor interfaces both at the QD-QD junctions and on the QD/graphene vdW interface. Ligand exchange provides a common solution to this problem by passivating the dangling chemical bonds on the QD surfaces. In the QD/graphene vdW heterostructures photodetectors, an additional role is required in ligand exchange for the ligand molecules to form efficient charge transport pathways at QD-QD and QD/graphene interfaces for high and fast photoresponse. For example, 3-mercaptopropionic acid (MPA) ligands have been found experimentally, as well as DFT simulation, to provide both passivation of the QDs and form the efficient charge transfer channels.<sup>16, 62</sup>

Another challenge in QD/graphene nanohybrids is associated to the limited light absorption by a thin layer (a monolayer or a few layer of QDs) of QDs in the nanohybrids. It should be noted increasing the QD thickness is not a good solution due to the limited QD-QD charge transport.<sup>18</sup> One scheme to address this issue is through coupling of plasmon nanostructures to the QD/graphene nanohybrids. For example, a plasmonic AgNPs-metafilm coupled with a thin (10-20 nm) insulating spacer to the nanohybrids has been found to enhance the photoresponse of the nanohybrid photodetectors

by  $>7$  times.<sup>65</sup> Core/shell QDs with plasmonic metal core wrapped with semiconductor shell provides another promising scheme.<sup>46</sup> An additional scheme for enhanced absorption as well as spectral tunability (red shift) is to make plasmonic QDs via carrier doping,<sup>52</sup> which has been found to not only provide remarkably enhanced light absorption by the QDs, but also the red shift of the cutoff much beyond the limit by the band gap into the IR spectrum. In comparison with the QDs of lower band gap semiconductors for IR detection, the plasmonic QDs of larger band gaps, such as iron pyrites<sup>66, 67</sup> (Eg in visible) and lead sulfites (Eg in NIR), have a unique advantage of much enhanced light absorption in broadband extended to IR spectrum, which allows much improved responsivity and  $D^*$  to be obtained in NIR-SWIR spectral range.

For the QD/graphene vdW heterostructures photodetectors, several different processes have been developed for fabrication of the vdW heterostructures nanohybrids. These processes can be divided into two types: direct growth using CVD or solution method, and mechanical stacking using drop-casting, spin-coating and inkjet printing. In both approaches, a control of the vdW interface is the key in achievement of the heterostructure nanohybrids for high-performance photodetectors and other optoelectronics since the interface provides the built-in field for exciton dissociation into free charge carriers and the follow-up charge transfer. Considering such a control must be at an atomic resolution, several post interface-cleaning processes have been explored including light-assisted vacuum annealing,<sup>68, 69</sup> ligand exchange,<sup>17, 70</sup> and ultrafast thermal annealing (UTA)<sup>71</sup>.

Light-assisted vacuum anneal could be operated at room temperature by placing the sample under illumination in vacuum typically  $\sim 10^{-6}$  Torr or better. A systematic shift of the Dirac point of graphene towards zero, which accelerates monotonically with increasing illumination time and intensity, has been observed during the annealing.<sup>69</sup> This confirms the removal of polar molecules adsorbed at the nanohybrid interface and their role as interface charge traps since a much enhanced photoresponse in both amplitude and speed was observed on the samples after the annealing. Ligand exchange has been extensively explored for replacing the ligands used in synthesis of QDs with ones that can provide better passivation of the QDs. In QDs/graphene nanohybrids, an additional consideration of the replacing ligand selection is their electrical conductivity for serving as the QD-QD (if a few QD layers are present) and QD/graphene charge transfer pathways. With adequate electric conduction, such ligands can lead to quench of the photoluminescence (PL), indicative of effective charge transfer out of QDs as required for QDs/graphene nanohybrids optoelectronics.<sup>17</sup> The UTA process exposes samples to high temperatures (up to 800 °C) for a short period of 1-3 seconds for refurbish the surface of the nanostructure sensitizers and their interfaces. For oxides nanohybrids, the UTA treatment in air was found to reduce the dark current and enhance photocurrent. In particular, graphene remains intact under the in-air UTA treatment.<sup>71</sup>

### 3. RESULT AND DISCUSSIONS

As we have mentioned earlier, the physical properties of graphene (such as carrier mobility) can be affected by molecules adsorbed on its surface during the graphene transfer and device fabrication processes, its interfaces with sensitizers and supporting substrates, the performance of the QD/graphene vdW heterostructure photodetectors would be sensitively dictated by them. Understanding the influence of these surface and interface factors on the QD/graphene vdW heterostructure photodetectors performance is therefore important. **Figure 2** illustrates several examples of the QD/graphene vdW heterostructure photodetectors that we have investigated towards such an understanding.<sup>68</sup> In **Figure 2a**, a III-V GaSe QDs/graphene vdW heterostructures photodetector is depicted schematically.<sup>68</sup> The interface built-in electric field anticipated from electronic structures of GaSe QD and graphene would result in hole transfer from GaSe to graphene. On the right, the dynamic photoresponse is compared for GaSe QDs/graphene vdW heterostructures photodetector without (**Figure 2b**) and with light-assisted vacuum annealing for  $>24$  hours (**Figure 2c**). Clear differences in both amplitude of the photoresponse and response times can be observed made with the annealing. In fact, the GaSe QDs printed on graphene channel often leads to an interface that may be contaminated by various chemicals, solvents and even air molecules used in the processing and printing of the GaSe-QDs, which can reduce the interface built-in electric field critical to exciton dissociation, block charge transfer across the interface and trap the charge to yield a slow response. The benefit of removing such an interface using the light-assisted vacuum annealing is clearly demonstrated in the enhanced dynamic photoresponse amplitude by up to three orders of magnitude.<sup>68</sup> This has yielded high gain or EQE in the range of  $10^7$ - $10^8$  and visible detectivity  $D^*$  up to  $7 \times 10^{13}$  Jones to visible light of 550 nm. In addition, faster and more symmetric photoresponse with 10-12 ms for both rise and fall time constants can be achieved simultaneously as compared to slower and asymmetric rise (18.5 ms) and fall (27 ms) before the cleaning, illustrating the charge traps at the vdW interface are detrimental to both photoresponse and response speed.

**Figures 2d-g** exhibit another example of ZnO QD/graphene vdW heterostructures photodetectors. ZnO has a bandgap in ultraviolet range (~340 nm) with a minor blue shift in ZnO QDs due to the size effect. However, an atomically thin Zn acetate surface layer may be present on the ZnO QDs (**Figure 2d**), which can behave like a charge blocking layer at the ZnO QD/graphene interface. Consequently, charge transfer from ZnO QDs to graphene can be blocked, which is illustrated in a negligible photoresponse to UV light. When this surface layer is systematically removed using an in-air aging process (**Figure 2e**), improved photoresponse by orders of magnitude can be obtained (**Figures 2f-g**).<sup>72</sup> In fact, the best responsivity up to  $9.9 \times 10^8$  A/W and  $D^*$  of  $\sim 10^{14}$  Jones to ultraviolet illumination at 340 nm in ZnO QD/graphene vdW heterostructures photodetectors with the removal of the Zn acetate surface demonstrates the critical importance of the surface and interface control at an atomic scale. It should be realized that such a control is not unique to the QD/graphene vdW heterostructures photodetectors. Even in the QDs-only photodetectors, this control is critical to enable a more efficient charge transport in QDs films in which massive QD-QD junctions are present as hurdles of the carrier transport. In a comparative study of ZnO QD film (QD diameter~ 20-40 nm) subjected to an UTA treatment to enable the formation of QD-QD interface nanojunctions, a nearly two orders of magnitude decrease of the dark current  $I_{\text{Dark}}$  and more than an order of magnitude increase of the photocurrent  $I_{\text{ph}}$  under ultraviolet illumination (340 nm). Moreover, a high  $I_{\text{ph}}/I_{\text{Dark}}$  ratio of  $3.1 \times 10^5$ , responsivity of up to  $430 \text{ A W}^{-1}$  at  $0.003 \text{ mW cm}^{-2}$ , detectivity of  $1.4 \times 10^{13}$  Jones were obtained. Interestingly, the UTA process can be applied to ZnO QD/graphene vdW heterostructures photodetectors for improved performance while graphene remains intact.<sup>63, 73</sup> Since the graphene channel of higher carrier mobility provides a more efficient charge transport pathway than the ZnO QD film with lower carrier mobility, the overall better performance of the ZnO QD/graphene vdW heterostructures photodetectors than their QDs-only counterparts' is well justified.

**Figures 2h-k** illustrate a third example of mixed PbS and FeS<sub>2</sub> QD/graphene vdW heterostructures broadband photodetector that relies on ligand exchange to improve the QD/graphene charge transfer. Ligand exchange provides an effective approach to passivate QD surface states and form an efficient charge transfer pathway from QD to graphene.<sup>13, 70, 72</sup> The PbS QDs of an average diameter of 4.3 nm have the optical cutoff at ~940 nm. FeS<sub>2</sub> has an extraordinary absorption coefficient up to  $6 \times 10^5 \text{ cm}^{-1}$ , which is 2 orders of magnitude higher than that of crystalline silicon. The FeS<sub>2</sub> QDs with doping have shown a strong light wavelength selectivity determined by their localized surface plasmon resonance (LSPR) frequency in near-IR to short-wave IR (NIR-SWIR) spectra.<sup>18, 19</sup> It is known that the LSPR frequency may be tuned by n- or p-doping of semiconductors of reasonable bandgaps that are large enough to not contribute substantial dark current at room temperature.<sup>52</sup> On the FeS<sub>2</sub> QD/graphene vdW heterostructures photodetectors, high responsivity up to  $8 \times 10^6$  A/W and  $D^*$  near  $10^{13}$  Jones have been demonstrated recently at NIR-SWIR.<sup>18, 19</sup> However, both PbS and FeS<sub>2</sub> QDs, like many other QDs for IR application, are synthesized in organic solutions. The as-synthesized QDs are capped with a layer of organic ligands of typically insulating (**Figure 2h**). While this capping layer protects the QDs in the colloidal form and would not affect the photoluminescence properties of the colloidal QDs, it blocks the charge transfer from QDs to graphene in the QD/graphene vdW heterostructures photodetectors. Ligand exchange is hence required to replace the insulating organic ligands with conducting ones. For the mixed PbS and FeS<sub>2</sub> QD/graphene vdW heterostructures broadband photodetectors, we have found that the 3-mercaptopropionic acid (MPA) ligands can replace the organic ligands from synthesis and provide highly efficient charge transfer pathway between the QDs to graphene (**Figure 2i**). Both photoresponse and response speed are improved by the MPA ligand exchange as shown in **Figures 2j-k** by almost three orders of magnitude, indicating insulating ligands may behave like charge traps at the QD/graphene interface. By using the mixed PbS and FeS<sub>2</sub> QDs with complimentary optical absorption spectra, an extraordinary photoresponsivity in exceeding  $\sim 10^6$  A/W was obtained in an broadband spectrum of ultraviolet-visible-NIR. In addition, the MPA ligand exchange has been found to passivate the QD surface against post-degradation in ambient. This benefit has been demonstrated in the CsPbCl<sub>3</sub> QDs/graphene vdW heterostructure photodetectors to improve the stability of the CsPbCl<sub>3</sub> QDs in ambient and the vdW heterojunction interface between CsPbCl<sub>3</sub> QDs and graphene, leading to a large photocurrent enhancement, up to three orders of magnitude improvement in response speed, and long term ambient stability.<sup>45, 46</sup>

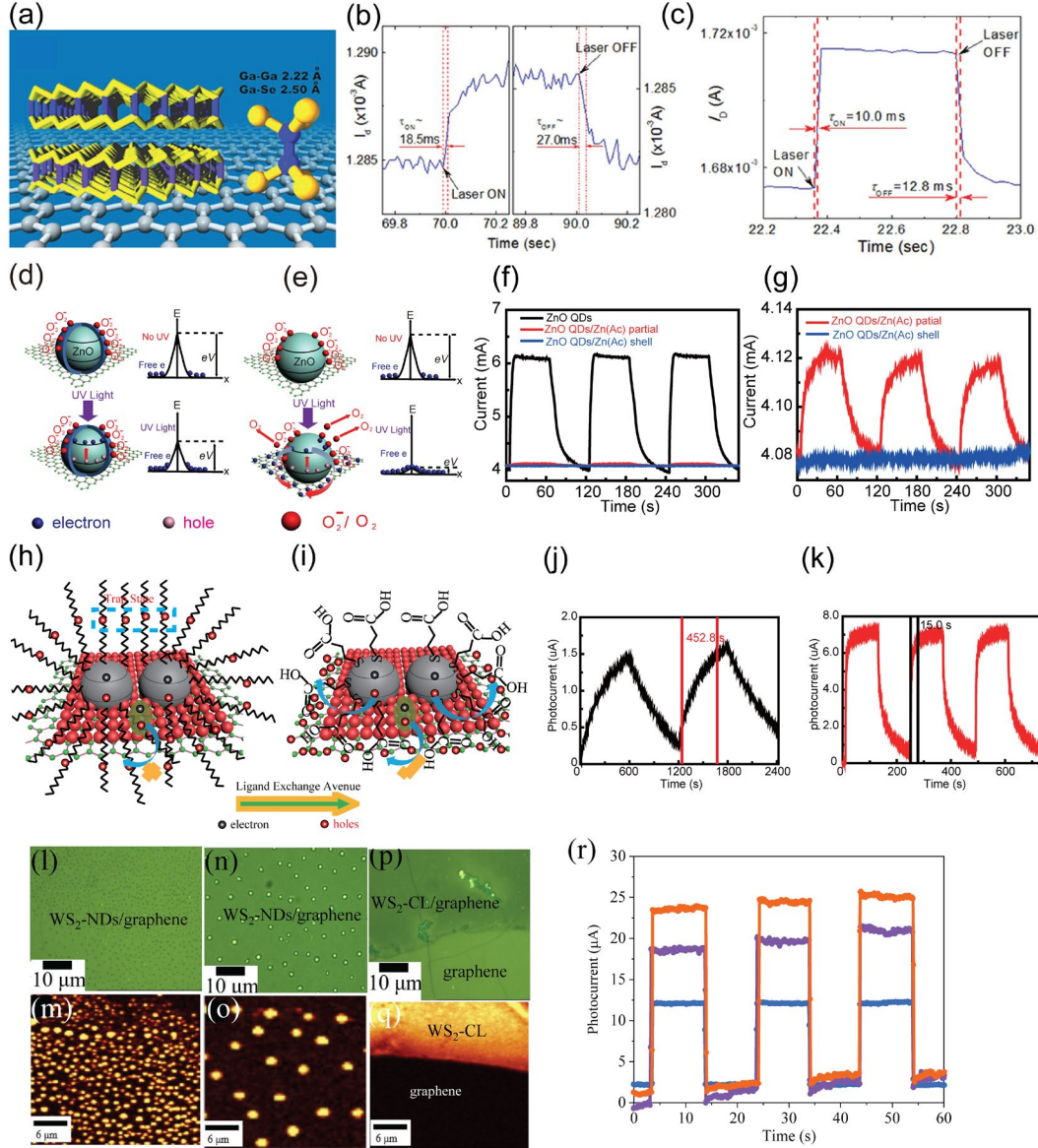


Figure 2. (a) The structure of GaSe nanosheet/graphene hybrid photodetector. The dynamic photocurrent of the device without (b) and with vacuum annealing (c). The band energy diagram with (d) and without (e) Zn(Ac) charge transfer blocking shell in dark and under illumination of UV light, associated with oxygen absorption/desorption and charge transfer process. (f) The dynamic photocurrent of ZnO QDs/graphene photodetector with and without Zn(Ac) blocking shell. (g) Zoom in the dynamic photocurrent on ZnO QDs with partial and full Zn(Ac) blocking shell. Schematics of a FeS<sub>2</sub>-PbS/GFET heterojunction and the corresponding charger transfer process before (h) and after (i) the ligand exchange. Dynamic photoresponse of FeS<sub>2</sub>-PbS/GFET photodetectors upon NIR illustration before ligand exchange (j) and after (k) the ligand exchange shown in (h) and (i), respectively. (l, n, p) Optical and (m, o, q) Raman mapping images of WS<sub>2</sub> with smaller and denser WS<sub>2</sub>-NDs in WS<sub>2</sub>-NDs/graphene (orange); larger and more dilute WS<sub>2</sub>-NDs WS<sub>2</sub>-NDs/graphene (purple) samples, and WS<sub>2</sub>-CL/graphene (blue). (r) The corresponding dynamic photocurrents measured in response to 550 nm light on and off as a function of the incident light intensity on the three devices.

**Figures 2l-r** exhibit the fourth example of QDs/graphene vdW heterostructure photodetectors obtained via layer-by-layer growth of TMDC QDs, or more accurately nanodiscs (NDs) of lateral dimension of hundreds of nm while vertical dimension of 3-7 nm.<sup>74-80</sup> CVD growth of QDs on graphene, such as TMDCs, allows layer-by-layer deposition in large area, which is important to the practical applications.<sup>74</sup> QDs/graphene vdW heterostructure photodetectors, a key benefit is a clean interface formed between TMDC and graphene, especially on transfer-free graphene. It is particularly worth

mentioned that the TMDC QDs are confirmed to LSPR and hence significantly enhanced light absorption/trapping due to a so-called photo-doping facilitated by the TMDC QD/graphene interface as suggested by a Density Function Theory simulation.<sup>76-78</sup> The benefit of these non-metal plasmonic nanostructures is in their inherent low loss. In fact, this argument is supported by the higher sensitivity of the TMDC-NDs/graphene, as compared with Au-NPs/graphene, in surface enhanced Raman spectroscopy of biomolecules, and higher responsivity in TMDC QDs/graphene photodetectors in comparison with the TMDC sheet/graphene counterpart's. For photodetection, an interesting difference has been observed on the response speeds of the TMDC QD/graphene vdW heterostructures photodetectors made with layer-by-layer growth<sup>76</sup> or with one or two transfer steps.<sup>79</sup> The response time is on the order of 10 ms in the former in contrast to >100 ms in the latter. This difference again demonstrates that a cleaner QD/graphene interface can be achieved in the layer-by-layer QD/graphene vdW heterostructures with much reduced charge traps that are detrimental to both photoresponse and response speed of the TMDC QD/graphene vdW heterostructures photodetectors.

While the layer-by-layer growth of the QD/graphene can lead to cleaner vdW interface required for high photoresponse and response speed, the method may not be applicable to many QDs since their growth conditions may not be suitable to graphene and could lead to degradation of graphene. An additional challenge is in the incompatibility of the QD/graphene growth condition to many technological important substrates such as plastics, polymers, metal sheets, etc. This means that post-cleaning methods are particularly suitable and useful when the QD/graphene vdW photodetectors or other devices are fabricated by inkjet printing of pre-synthesized colloidal QDs on graphene. In fact, printing with inks of pre-fabricated crystalline QDs<sup>15, 72</sup> or precursors that only require a moderate thermal budget<sup>64, 81</sup> could provide a promising approach for integration of QD/graphene vdW heterostructures photodetectors or imaging arrays with complementary metal oxide semiconductors.<sup>82</sup>

**Tables 1** summarizes some representative results of QDs/graphene vdW heterostructure nanohybrids for infrared detection. Overall, the performance is promising. For instance, Konstantatos *et al* reported a PbS QD/graphene vdW heterostructures photodetectors with a layer of PbS QDs spin-coated on graphene channel.<sup>13, 83</sup> At wavelengths near 1.55  $\mu\text{m}$ ,  $D^*$  as high as  $10^{12}$  Jones, which is comparable to the current state of the arts conventional III-V semiconductor uncooled IR detectors at comparable wavelengths (<1.7  $\mu\text{m}$ ). However, the performance limitation of the conventional uncooled IR detectors stems fundamentally from the low bandgaps of the semiconductors employed. Since the signal to noise ratio decreases with the bandgap, cooling become mandatory to maintain high  $D^*$  at the level of  $10^{12}$  Jones beyond 1.7  $\mu\text{m}$  wavelengths. In contrast, the promising results obtained on QDs/graphene vdW heterostructures suggest a large room for further enhancement of the IR detector performance via understanding of the underlying device physics and optimization of the device design parameters.

**Table 1.** Performance of some representative QDs/graphene vdW heterostructures nanohybrid for infrared detection.

QD material	Spectrum	Cutoff wavelength ( $\mu\text{m}$ )	R (A/W)	$D^*$ (Jones)	Response time (s)	Ref.
PbS	Vis-SWIR	>1.8	-	$10^{12}$ (at 1.55 $\mu\text{m}$ )	$10^{-2}$	83, 84
Ti <sub>2</sub> O <sub>3</sub>	MWIR-LWIR	10	>120	$7 \times 10^8$ (at 10 $\mu\text{m}$ )	$10^{-3}$	85
HgTe	SWIR	1.55	$6 \times 10^{-3}$	$10^9$ (at 1.55 $\mu\text{m}$ )	$9 \times 10^{-6}$	86
HgTe	NIR-MIR	>3	$10^2$	$6 \times 10^8$ (at 2.5 $\mu\text{m}$ )	$7 \times 10^{-4}$	87
Si (B-doped)	UV-MIR	3.9	10	$10^5$ (at 3 $\mu\text{m}$ )	-	88
PbSe nanorods	NIR-MIR	3	7.6	-	$2.8 \times 10^{-4}$	89
FeS <sub>2</sub> -PbS	UV-NIR	>1.1	> $10^6$	> $10^{11}$	3.5	16
FeS <sub>2</sub>	UV-NIR	>1.1	> $10^6$	> $10^{12}$	0.1	18



## 4. CONCLUSIONS

In summary, QDs/graphene vdW heterostructure photodetectors have recently emerged as a unique scheme for high-performance uncooled photodetection, particularly in IR spectra. It should be realized that the QDs/graphene vdW heterostructures are quantum devices relying on the strong quantum confinement in QDs for spectral tunability and reduced dark current due to suppressed phonon scattering, and in graphene for extraordinary carrier mobility. This can lead to high photoconductive gain or EQE as demonstrated experimentally in various QDs/graphene vdW heterostructure photodetectors for a broad spectral range from ultraviolet to IR. Nevertheless, research on QDs/graphene vdW heterostructure photodetectors, especially for IR detection, has just begun and many important issues remain. Specifically, QDs have a high surface to volume ratio and the large amount of the surface area demand a careful control of the QD surface states (growth defects, dangling bonds, impurity layer, adsorbed species, etc) to eliminate charge traps that can reduce both photoresponse and response speed dramatically. This surface state issue will be particularly important in QDs of small bandgaps for IR detectors. In line with this, a precise control of the QD/graphene interface to eliminate charge transfer blocking layer and charge traps is critically important to achieving the anticipated high photoresponse and response speed, both are critical to commercial IR detectors and imaging systems. This calls for development of new approaches to achieve an atomic control on these surfaces and interfaces and will be a focus of future research on QDs/graphene vdW heterostructure IR detectors.

## ACKNOWLEDGEMENTS

This research was supported in part by ARO Contract No. ARO-W911NF-16-1-0029 and NSF Contract Nos. NSF-ECCS-1809293, NSF-DMR-1909292, and NSF-DMR-1508494.

## REFERENCE

1. K. S. Novoselov, A. K. Geim, S. V. Morozov, D. Jiang, Y. Zhang, S. V. Dubonos, I. V. Grigorieva and A. A. Firsov, "Electric field effect in atomically thin carbon films", *Science* **306** (5296), 666-669 (2004).
2. A. K. Geim and K. S. Novoselov, "The rise of graphene", *Nature Materials* **6** (3), 183-191 (2007).
3. K. S. Novoselov, A. K. Geim, S. V. Morozov, D. Jiang, Y. Zhang, S. V. Dubonos, I. V. Grigorieva and A. A. Firsov, "Electric field effect in atomically thin carbon films", *Science* **306** (5696), 666-669 (2004).
4. K. S. Novoselov, A. K. Geim, S. V. Morozov, D. Jiang, M. I. Katsnelson, I. V. Grigorieva, S. V. Dubonos and A. A. Firsov, "Two-dimensional gas of massless Dirac fermions in graphene", *Nature* **438** (7065), 197-200 (2005).
5. Y. B. Zhang, Y. W. Tan, H. L. Stormer and P. Kim, "Experimental observation of the quantum Hall effect and Berry's phase in graphene", *Nature* **438** (7065), 201-204 (2005).
6. P. Avouris, Z. H. Chen and V. Perebeinos, "Carbon-based electronics", *Nat. Nanotechnol.* **2** (10), 605-615 (2007).
7. C. R. Dean, A. F. Young, I. Meric, C. Lee, L. Wang, S. Sorgenfrei, K. Watanabe, T. Taniguchi, P. Kim, K. L. Shepard and J. Hone, "Boron nitride substrates for high-quality graphene electronics", *Nat. Nanotechnol.* **5** (10), 722-726 (2010).
8. J. H. Chen, C. Jang, S. D. Xiao, M. Ishigami and M. S. Fuhrer, "Intrinsic and extrinsic performance limits of graphene devices on SiO<sub>2</sub>", *Nat. Nanotechnol.* **3** (4), 206-209 (2008).
9. A. K. Geim, "Graphene: Status and Prospects", *Science* **324** (5934), 1530-1534 (2009).
10. R. R. Nair, P. Blake, A. N. Grigorenko, K. S. Novoselov, T. J. Booth, T. Stauber, N. M. R. Peres and A. K. Geim, "Fine structure constant defines visual transparency of graphene", *Science* **320** (5881), 1308-1308 (2008).
11. X. S. Li, W. W. Cai, J. H. An, S. Kim, J. Nah, D. X. Yang, R. Piner, A. Velamakanni, I. Jung, E. Tutuc, S. K. Banerjee, L. Colombo and R. S. Ruoff, "Large-Area Synthesis of High-Quality and Uniform Graphene Films on Copper Foils", *Science* **324** (5932), 1312-1314 (2009).
12. J. Z. Wu, "Graphene", in *Transparent Conductive Materials. Materials, Synthesis and Characterization*, edited by D. L. a. D. E. Castellón (Wiley-VCH, 2019), Vol. Vol. 1 & 2, pp. 165-192.



13. G. Konstantatos, M. Badioli, L. Gaudreau, J. Osmond, M. Bernechea, F. P. G. de Arquer, F. Gatti and F. H. L. Koppens, "Hybrid graphene-quantum dot phototransistors with ultrahigh gain", *Nat. Nanotechnol.* **7** (6), 363-368 (2012).
14. A. K. Geim and I. V. Grigorieva, "Van der Waals heterostructures", *Nature* **499** (7459), 419-425 (2013).
15. M. Gong, Liu, Qingfeng, Cook, Brent, Ewing, Daniel, Casper, Matthew, Stramel, Wu, Judy "All-printable ZnO quantum dots/Graphene van der Waals heterostructures for ultrasensitive detection of ultraviolet light", *ACS nano* **11** (4), 4114 (2017).
16. M. Gong, Q. Liu, R. Goul, D. Ewing, M. Casper, A. Stramel, A. Elliot and J. Z. Wu, "Printable Nanocomposite FeS<sub>2</sub>-PbS Nanocrystals / Graphene Heterojunction Photodetectors for Broadband Photodetection", *ACS Appl Mater Interfaces* **9**, 27801–27808 (2017).
17. M. G. Gong, R. Sakidja, R. Goul, D. Ewing, M. Casper, A. Stramel, A. Elliot and J. Z. Wu, "High-Performance All-Inorganic CsPbCl<sub>3</sub> Perovskite Nanocrystal Photodetectors with Superior Stability", *Acs Nano* **13** (2), 1772-1783 (2019).
18. M. Gong, D. Ewing, M. Casper, A. Stramel, A. Elliot and J. Z. Wu, "Controllable Synthesis of Monodispersed Fe<sub>1-x</sub>S<sub>2</sub> Nanocrystals for High-Performance Optoelectronic Devices", *ACS Appl Mater Interfaces* **11** (21), 19286-19293 (2019).
19. M. Gong, R. Sakidja, Q. Liu, R. Goul, D. Ewing, M. Casper, A. Stramel, A. Elliot and J. Z. Wu, "Broadband Photodetectors: Broadband Photodetectors Enabled by Localized Surface Plasmonic Resonance in Doped Iron Pyrite Nanocrystals (Advanced Optical Materials 8/2018)", *Advanced Optical Materials* **6** (8), 1870033 (2018).
20. B. Cook, Q. F. Liu, J. W. Liu, M. G. Gong, D. Ewing, M. Casper, A. Stramel and J. D. Wu, "Facile zinc oxide nanowire growth on graphene via a hydrothermal floating method: towards Debye length radius nanowires for ultraviolet photodetection", *Journal of Materials Chemistry C* **5** (38), 10087-10093 (2017).
21. J. Liu, R. Lu, G. Xu, J. Wu, P. Thapa and D. Moore, "Development of a Seedless Floating Growth Process in Solution for Synthesis of Crystalline ZnO Micro/Nanowire Arrays on Graphene: Towards High - Performance Nanohybrid Ultraviolet Photodetectors", *Advanced Functional Materials* **23** (39), 4941-4948 (2013).
22. F. Xia, H. Wang, D. Xiao, M. Dubey and A. Ramasubramaniam, "Two-dimensional material nanophotonics", *Nature Photonics* **8**, 899-907 (2014).
23. K. Roy, M. Padmanabhan, S. Goswami, T. P. Sai, G. Ramalingam, S. Raghavan and A. Ghosh, "Graphene–MoS<sub>2</sub> hybrid structures for multifunctional photoresponsive memory devices", *Nat. Nanotechnol.* **8**, 826-830 (2013).
24. F. P. García de Arquer, A. Armin, P. Meredith and E. H. Sargent, "Solution-processed semiconductors for next-generation photodetectors", *Nature Reviews Materials* **2** (3), 16100 (2017).
25. S. De and J. N. Coleman, "Are There Fundamental Limitations on the Sheet Resistance and Transmittance of Thin Graphene Films?", *Acs Nano* **4** (5), 2713-2720 (2010).
26. S. Stankovich, D. A. Dikin, G. H. B. Dommett, K. M. Kohlhaas, E. J. Zimney, E. A. Stach, R. D. Piner, S. T. Nguyen and R. S. Ruoff, "Graphene-based composite materials", *Nature* **442** (7100), 282-286 (2006).
27. R. R. Nair, P. Blake, A. N. Grigorenko, K. S. Novoselov, T. J. Booth, T. Stauber, N. M. Peres and A. K. Geim, "Fine structure constant defines visual transparency of graphene", *Science* **320** (5881), 1308 (2008).
28. U. Bockelmann, "ELECTRONIC RELAXATION IN QUASI-ONE-DIMENSIONAL AND ZERO-DIMENSIONAL STRUCTURES", *Semiconductor Science and Technology* **9** (5), 865-870 (1994).
29. D. M. T. Kuo, A. B. Fang and Y. C. Chang, "Theoretical modeling of dark current and photo-response for quantum well and quantum dot infrared detectors", *Infrared Physics & Technology* **42** (3-5), 433-442 (2001).
30. V. J. Logeeswaran, J. Oh, A. P. Nayak, A. M. Katzenmeyer, K. H. Gilchrist, S. Grego, N. P. Kobayashi, S. Y. Wang, A. A. Talin, N. K. Dhar and M. S. Islam, "A Perspective on Nanowire Photodetectors: Current Status, Future Challenges, and Opportunities", *Ieee Journal of Selected Topics in Quantum Electronics* **17** (4), 1002-1032 (2011).
31. S. Keuleyan, E. Lhuillier, V. Brajuskovic and P. Guyot-Sionnest, "Mid-infrared HgTe colloidal quantum dot photodetectors", *Nature Photonics* **5** (8), 489-493 (2011).
32. S. Keuleyan, E. Lhuillier and P. Guyot-Sionnest, "Synthesis of Colloidal HgTe Quantum Dots for Narrow Mid-IR Emission and Detection", *Journal of the American Chemical Society* **133** (41), 16422-16424 (2011).
33. E. Lhuillier, S. Keuleyan, P. Rekemeyer and P. Guyot-Sionnest, "Thermal properties of mid-infrared colloidal quantum dot detectors", *Journal of Applied Physics* **110** (3) (2011).
34. H. Chen, X. Sun, K. W. C. Lai, M. Meyyappan and N. Xi, "Infrared Detection Using an InSb Nanowire", in *2009 IEEE Nanotechnology Materials and Devices Conference* (Traverse City, Michigan, USA, 2009), pp. 212.
35. M. I. Khan, X. Wang, X. Y. Jing, K. N. Bozhilov and C. S. Ozkan, "Study of a Single InSb Nanowire Fabricated via DC Electrodeposition in Porous Templates", *Journal of Nanoscience and Nanotechnology* **9** (4), 2639-2644 (2009).

36. J. W. Liu, R. T. Lu, G. W. Xu, J. Wu, P. Thapa and D. Moore, "Development of a Seedless Floating Growth Process in Solution for Synthesis of Crystalline ZnO Micro/Nanowire Arrays on Graphene: Towards High-Performance Nanohybrid Ultraviolet Photodetectors", *Advanced Functional Materials* **23** (39), 4941-4948 (2013).
37. R. T. Lu, Liu, J. W., Luo, H. F., Chikan, V., and Wu, J. Z., "Graphene/GaSe-Nanosheet Hybrid: Towards High Gain and Fast Photoresponse", *Scientific Reports* **6**, 19161 (2016).
38. Q. F. Liu, Cook, B., Gong, M.G., Gong, Y.P., Ewing, D., Casper, M., Stramel, A., Wu, J.Z., "Transfer-Free Fabrication of Two-Dimensional MoS<sub>2</sub>/Graphene Heterostructures on SiO<sub>2</sub>/Si Substrates for High-Performance and Scalable Photodetectors", *Acs Appl Mater Inter* **9** (14), 12728 (2017).
39. A. Rogalski, *Infrared Detectors (Second Edition)*. (CRC Press, Boca Raton, FL, 2011).
40. S. Roy, A. Aguirre, D. A. Higgins and V. Chikan, "Investigation of Charge Transfer Interactions in CdSe Nanorod P3HT/PMMA Blends by Optical Microscopy", *Journal of Physical Chemistry C* **116** (4), 3153-3160 (2012).
41. W. J. Zhang, C. P. Chuu, J. K. Huang, C. H. Chen, M. L. Tsai, Y. H. Chang, C. T. Liang, Y. Z. Chen, Y. L. Chueh, J. H. He, M. Y. Chou and L. J. Li, "Ultrahigh-Gain Photodetectors Based on Atomically Thin Graphene-MoS<sub>2</sub> Heterostructures", *Scientific Reports* **4**, 3826 (2014).
42. W. J. Zhang, J. K. Huang, C. H. Chen, Y. H. Chang, Y. J. Cheng and L. J. Li, "High-Gain Phototransistors Based on a CVD MoS<sub>2</sub> Monolayer", *Advanced Materials* **25** (25), 3456-3461 (2013).
43. R. T. Lu, Liu, J. W., Luo, H. F., Chikan, V., and Wu, J. Z., "Ligand-Free Graphene/GaSe-Nanosheet Hybrid: Towards High Gain and Fast Photoresponse", *submitted*. (2015).
44. M. Gong, Liu, Qingfeng, Cook, Brent, Ewing, Daniel, Casper, Matthew, Stramel, Wu, Judy "All-printable ZnO quantum dots/Graphene van der Waals heterostructures for ultrasensitive detection of ultraviolet light, ASAP", *ACS NANO, ASAP* (2017).
45. M. Gong, R. Sakidja, R. Goul, D. Ewing, M. Casper, A. Stramel, A. Elliot and J. Z. Wu, "High-Performance All-Inorganic CsPbCl<sub>3</sub> Perovskite Nanocrystal Photodetectors with Superior Stability", *ACS Nano* **13** (2), 1772-1783 (2019).
46. M. Gong, M. Alamri, D. Ewing, S. M. Sadeghi and J. Z. Wu, "Localized Surface Plasmon Resonance Enhanced Light Absorption in AuCu/CsPbCl<sub>3</sub> Core/Shell Nanocrystals", *Advanced Materials* **32** (26), 2002163 (2020).
47. E. L. Dereniak and G. D. Boreman, *Infrared Detectors and Systems*. (John Willey & Sons., New York, USA, 1996).
48. J. Caniou, *Passive Infrared Detection-Theory and Applications* (Kluwer Academic, Boston, USA, 1999).
49. M. Henini and M. Razeghi, *Handbook of Infrared Detection Technologies*. (Elsevier Science, New York, 2002).
50. M. A. Kinch, *Fundamentals of Infrared Detector Materials* (SPIE Press., Washington, USA, 2007).
51. H. Lu, G. M. Carroll, N. R. Neale and M. C. Beard, "Infrared Quantum Dots: Progress, Challenges, and Opportunities", *ACS Nano* **13** (2), 939-953 (2019).
52. J. M. Luther, P. K. Jain, T. Ewers and A. P. Alivisatos, "Localized surface plasmon resonances arising from free carriers in doped quantum dots", *Nature Materials* **10** (5), 361-366 (2011).
53. J. Wu, Y. Lu, S. Feng, Z. Wu, S. Lin, Z. Hao, T. Yao, X. Li, H. Zhu and S. Lin, "The Interaction between Quantum Dots and Graphene: The Applications in Graphene - Based Solar Cells and Photodetectors", *Advanced Functional Materials* **28** (50) (2018).
54. J. Z. Wu, and Gong, M.G., "Invited Review: Nanohybrid Photodetectors", *Advanced Photonics Research* (2021 (under revision)).
55. J. Z. Wu, Gong, M.G., Schmitz, R.C., Liu, B., , "(invited book chapter) Quantum Dot/Graphene Heterostructure Nanohybrid Photodetectors", *Springer-Nature Book Series: Lecture Notes in Nanoscale Science and Technology* (2021 (under revision)).
56. Q. F. Liu, Y. P. Gong, J. S. Wilt, R. Sakidja and J. Wu, "Synchronous growth of AB-stacked bilayer graphene on Cu by simply controlling hydrogen pressure in CVD process", *Carbon* **93**, 199-206 (2015).
57. J. Liu, G. Xu, C. Rochford, R. Lu, J. Wu, C. M. Edwards, C. L. Berrie, Z. Chen and V. A. Maroni, "Doped graphene nanohole arrays for flexible transparent conductors", *Applied Physics Letters* **99** (2), 023111 (2011).
58. G. W. Xu, R. T. Lu, J. W. Liu, H. Y. Chiu, R. Q. Hui and J. Z. Wu, "Photodetection Based on Ionic Liquid Gated Plasmonic Ag Nanoparticle/Graphene Nanohybrid Field Effect Transistors", *Advanced Optical Materials* **2** (8), 729-736 (2014).
59. Q. Liu, Y. Gong, T. Wang, W.-L. Chan and J. Wu, "Metal-catalyst-free and controllable growth of high-quality monolayer and AB-stacked bilayer graphene on silicon dioxide", *Carbon* **96**, 203-211 (2016).

60. M. Panth, B. Cook, M. Alamri, D. Ewing, A. Wilson and J. Z. Wu, "Flexible Zinc Oxide Nanowire Array/Graphene Nanohybrid for High-Sensitivity Strain Detection", *ACS Omega* **5** (42), 27359-27367 (2020).
61. G. Xu, R. Lu, J. Liu, H.-Y. Chiu, R. Hui and J. Wu, "Photodetection based on Ionic Liquid Gated Plasmonic Ag Nanoparticle/ Graphene Nanohybrid Field Effect Transistors", *Advanced Optical Materials* **2** (8), 729-736 (2014).
62. M. Gong, A. Kirkeminde, Y. Xie, R. Lu, J. Liu, J. Wu and S. Q. Ren, "Iron Pyrite (FeS<sub>2</sub>) Broad Spectral and Magnetically Responsive Photodetectors", *Advanced Optical Materials* **1**, 78-83 (2013).
63. B. Cook, M. Gong, D. Ewing, M. Casper, A. Stramel, A. Elliot and J. Wu, "Inkjet Printing Multicolor Pixelated Quantum Dots on Graphene for Broadband Photodetection", *ACS Applied Nano Materials* **2** (5), 3246-3252 (2019).
64. B. Cook, Q. F. Liu, M. G. Gong, D. Ewing, M. Casper, A. Stramel and J. Wu, "Quantum Dots-Facilitated Printing of ZnO Nanostructure Photodetectors with Improved Performance", *Acs Appl Mater Inter* **9** (27), 23189-23194 (2017).
65. B. Liu, R. R. Gutha, B. Kattel, M. Alamri, M. Gong, S. M. Sadeghi, W.-L. Chan and J. Z. Wu, "Using Silver Nanoparticles-Embedded Silica Metafilms as Substrates to Enhance the Performance of Perovskite Photodetectors", *Acs Appl Mater Inter* **11** (35), 32301-32309 (2019).
66. M. Gong, A. Kirkeminde, N. Kumar, H. Zhao and S. Ren, "Ionic-passivated FeS<sub>2</sub> photocapacitors for energy conversion and storage", *Chem. Commun.* **49** (81), 9260-9262 (2013).
67. M. Gong, A. Kirkeminde and S. Ren, "Symmetry-defying iron pyrite (FeS<sub>2</sub>) nanocrystals through oriented attachment", *Sci Rep* **3**, 2092 (2013).
68. R. T. Lu, J. W. Liu, H. F. Luo, V. Chikan and J. Z. Wu, "Graphene/GaSe-Nanosheet Hybrid: Towards High Gain and Fast Photoresponse", *Scientific Reports* **6**, 19161 (2016).
69. Y. Zhang, G. Hu, M. Gong, M. Alamri, C. Ma, M. Liu and J. Z. Wu, "Lateral Graphene p-n Junctions Realized by Nanoscale Bipolar Doping Using Surface Electric Dipoles and Self-Organized Molecular Anions", *Advanced Materials Interfaces* **6** (1), 1801380 (2019).
70. M. G. Gong, Q. F. Liu, R. Goul, D. Ewing, M. Casper, A. Stramel, A. Elliot and J. Z. Wu, "Printable Nanocomposite FeS<sub>2</sub>-PbS Nanocrystals/Graphene Heterojunction Photodetectors for Broadband Photodetection", *Acs Appl Mater Inter* **9** (33), 27801-27808 (2017).
71. Q. Liu, M. Gong, B. Cook, D. Ewing, M. Casper, A. Stramel and J. Wu, "Fused Nanojunctions of Electron - Depleted ZnO Nanoparticles for Extraordinary Performance in Ultraviolet Detection", *Advanced Materials Interfaces* (2017).
72. M. Gong, Q. Liu, B. Cook, B. Kattel, T. Wang, W. L. Chan, D. Ewing, M. Casper, A. Stramel and J. Z. Wu, "All-Printable ZnO Quantum Dots/Graphene van der Waals Heterostructures for Ultrasensitive Detection of Ultraviolet Light", *ACS Nano* **11**, 4114-4123 (2017).
73. B. Cook, M. Gong, A. Corbin, D. Ewing, A. Tramble and J. Wu, "Inkjet-Printed Imbedded Graphene Nanoplatelet/Zinc Oxide Bulk Heterojunctions Nanocomposite Films for Ultraviolet Photodetection", *ACS Omega* **4** (27), 22497-22503 (2019).
74. Q. F. Liu, B. Cook, M. G. Gong, Y. P. Gong, D. Ewing, M. Casper, A. Stramel and J. D. Wu, "Printable Transfer-Free and Wafer-Size MoS<sub>2</sub>/Graphene van der Waals Heterostructures for High-Performance Photodetection", *Acs Appl Mater Inter* **9** (14), 12728-12733 (2017).
75. M. Alamri, R. Sakidja, R. Goul, S. Ghopry and J. Z. Wu, "Plasmonic Au Nanoparticles on 2D MoS<sub>2</sub>/Graphene van der Waals Heterostructures for High-Sensitivity Surface-Enhanced Raman Spectroscopy", *ACS Applied Nano Materials* **2** (3), 1412-1420 (2019).
76. M. Alamri, M. Gong, B. Cook, R. Goul and J. Z. Wu, "Plasmonic WS<sub>2</sub> Nanodiscs/Graphene van der Waals Heterostructure Photodetectors", *Acs Appl Mater Inter* **11** (36), 33390-33398 (2019).
77. S. A. Ghopry, M. A. Alamri, R. Goul, R. Sakidja and J. Z. Wu, "Extraordinary Sensitivity of Surface-Enhanced Raman Spectroscopy of Molecules on MoS<sub>2</sub> (WS<sub>2</sub>) Nanodomains/Graphene van der Waals Heterostructure Substrates", *Advanced Optical Materials* **7** (8), 1801249 (2019).
78. S. A. Ghopry, M. Alamri, R. Goul, B. Cook, S. M. Sadeghi, R. R. Gutha, R. Sakidja and J. Z. Wu, "Au Nanoparticle/WS<sub>2</sub> Nanodome/Graphene van der Waals Heterostructure Substrates for Surface-Enhanced Raman Spectroscopy", *ACS Applied Nano Materials* **3** (3), 2354-2363 (2020).
79. M. Alamri, B. Liu, S. M. Sadeghi, D. Ewing, A. Wilson, J. L. Doolin, C. L. Berrie and J. Wu, "Graphene/WS<sub>2</sub> Nanodisk Van der Waals Heterostructures on Plasmonic Ag Nanoparticle-Embedded Silica Metafilms for High-Performance Photodetectors", *ACS Applied Nano Materials* **3** (8), 7858-7868 (2020).

80. S. A. Ghopry, S. M. Sadeghi, Y. Farhat, C. L. Berrie, M. Alamri and J. Z. Wu, "Intermixed WS<sub>2</sub>+MoS<sub>2</sub> Nanodisks/Graphene van der Waals Heterostructures for Surface-Enhanced Raman Spectroscopy Sensing", *ACS Applied Nano Materials* **4** (3), 2941-2951 (2021).
81. Q. F. Liu, M. G. Gong, B. Cook, D. Ewing, M. Casper, A. Stramel and J. Wu, "Transfer-free and printable graphene/ZnO-nanoparticle nanohybrid photodetectors with high performance", *Journal of Materials Chemistry C* **5** (26), 6427-6432 (2017).
82. J. Kim, R. Kumar, A. J. Bandothkar and J. Wang, "Advanced Materials for Printed Wearable Electrochemical Devices: A Review", *Adv Electron Mater* **3** (1) (2017).
83. G. Konstantatos, M. Badioli, L. Gaudreau, J. Osmond, M. Bernechea, F. P. Garcia de Arquer, F. Gatti and F. H. Koppens, "Hybrid graphene-quantum dot phototransistors with ultrahigh gain", *Nat Nanotechnol* **7** (6), 363-368 (2012).
84. S. Goossens, G. Navickaite, C. Monasterio, S. Gupta, J. J. Piqueras, R. Pérez, G. Burwell, I. Nikitskiy, T. Lasanta, T. Galán, E. Puma, A. Centeno, A. Pesquera, A. Zurutuza, G. Konstantatos and F. Koppens, "Broadband image sensor array based on graphene-CMOS integration", *Nature Photonics* **11** (6), 366-371 (2017).
85. X. Yu, Y. Li, X. Hu, D. Zhang, Y. Tao, Z. Liu, Y. He, M. A. Haque, Z. Liu, T. Wu and Q. J. Wang, "Narrow bandgap oxide nanoparticles coupled with graphene for high performance mid-infrared photodetection", *Nat Commun* **9** (1), 4299 (2018).
86. U. N. Nounbe, C. Greboval, C. Livache, A. Chu, H. Majjad, L. E. Parra Lopez, L. D. N. Mouafo, B. Doudin, S. Berciaud, J. Chaste, A. Ouerghi, E. Lhuillier and J. F. Dayen, "Reconfigurable 2D/0D p-n Graphene/HgTe Nanocrystal Heterostructure for Infrared Detection", *ACS Nano* **14** (4), 4567-4576 (2020).
87. M. J. Grotevent, C. U. Hail, S. Yakunin, D. Bachmann, M. Calame, D. Poulidakos, M. V. Kovalenko and I. Shorubalko, "Colloidal HgTe Quantum Dot/Graphene Phototransistor with a Spectral Sensitivity Beyond 3  $\mu\text{m}$ ", *Advanced Science* (2021).
88. Z. Ni, L. Ma, S. Du, Y. Xu, M. Yuan, H. Fang, Z. Wang, M. Xu, D. Li, J. Yang, W. Hu, X. Pi and D. Yang, "Plasmonic Silicon Quantum Dots Enabled High-Sensitivity Ultrabroadband Photodetection of Graphene-Based Hybrid Phototransistors", *ACS Nano* **11** (10), 9854-9862 (2017).
89. H. Talebi, M. Dolatyari, G. Rostami, A. Manzuri, M. Mahmudi and A. Rostami, "Fabrication of fast mid-infrared range photodetector based on hybrid graphene-PbSe nanorods", *Appl Opt* **54** (20), 6386-6390 (2015).